Journal of Instrumentation

Experimental investigation of new ultra-lightweight support and cooling structures for the new Inner Tracking System of the ALICE Detector

Published by IOP Publishing for Sissa Medialab

Received: *April 3, 2018*
Revised: *June 6, 2018*
Accepted: *July 25, 2018*
Published: *August 3, 2018*

TECHNICAL REPORT

Experimental investigation of new ultra-lightweight support and cooling structures for the new Inner Tracking System of the ALICE Detector

V.I. Zherebchevsky,[a,1] **I.G. Altsybeev,**[a] **G.A. Feofilov,**[a] **A. Francescon,**[b] **C. Gargiulo,**[b] **S.N. Igolkin,**[a,b] **E.B. Krymov,**[a] **E. Laudi,**[b] **T.V. Lazareva,**[a] **N.A. Maltsev,**[a] **M. Gomez Marzoa,**[b,c] **N.A. Prokofiev**[a] **and D.G. Nesterov**[a]

[a] *St.-Petersburg State University, 7-9, Universitetskaya nab., St.-Petersburg, 199034, Russia*
[b] *European Organization for Nuclear Research, CERN, CH-1211 Geneva 23, Switzerland*
[c] *Laboratoire de Transfert de Chaleur et de Masse (LTCM), École Polytechnique Fédérale de Lausanne (EPFL), Route Cantonale,1015 Lausanne, Switzerland*

E-mail: v.zherebchevsky@spbu.ru

Abstract: Thermal cooling performances of extremely lightweight mechanical carbon fiber support structures with an integrated liquid cooling system for monolithic silicon pixel detectors have been investigated. The high heat removal efficiency using single-phase liquid flow is shown for a power density up to 0.5 W/cm^2. These solutions provide therefore possibility to build a detector with a record radiation length of 0.3% per layer, ensuring considerable extensions of the physical program of investigations of the quark-gluon plasma in ultra-relativistic heavy-ion collisions at the Large Hadron Collider.

Keywords: Detector cooling and thermo-stabilization; Overall mechanics design (support structures and materials, vibration analysis etc); Particle tracking detectors

[1] Corresponding author.

https://doi.org/10.1088/1748-0221/13/08/T08003

2018 JINST 13 T08003

Contents

1 Introduction

The upcoming modernization of ALICE (A Large Ion Collider Experiment) [1, 2] is motivated by new physics goals that could be reached after the next stage of the LHC (Large Hadron Collider) upgrade. This includes measurements of the heavy-flavor yields (of particles containing c and b quarks), their diffusion coefficients, thermalization processes and mass dependence, azimuthal anisotropy, as well as the study of thermal dileptons and charmonium yields at very low transverse momenta, investigations of the space-time evolution of the QGP. To achieve these goals, it is critical to improve the spatial resolution of secondary vertices and to decrease a registration threshold for transverse momenta of charged particles. Therefore, new high granularity detectors should be used for tracking of charged particles providing minimal distortions due to multiple scattering effects. These requirements are among the main conditions for the future ALICE upgrade.

A key role in determining coordinates of secondary vertices in ALICE belongs to the Inner Tracking System (ITS), the central vertex detector surrounding the interaction point. The modernization strategy of the ITS [1, 2] aims to realize experimental studies with the LHC beams after the year 2020, when the luminosity of the collider will be increased almost tenfold.

The general increase of multiplicity of charged particles is expected in Pb-Pb collisions after the LHC upgrade. This imposes, along with the high detector granularity, tight requirements on the speed of new detectors to be used in the upgrade.

A new type of complementary metal oxide semiconductor (CMOS) technology (180 nm CMOS Imaging Sensor process of TowerJazz) has been selected for the modernized ALICE ITS. A typical intrinsic feature of such detectors is the high level of integration of the front-end readout electronics into these solid state devices. As a result, depending on the electronics design and on the energy density dissipation the pixel detectors in the ITS require an efficient heat sink in order to ensure the operation of electronics and detector at a temperature not higher than 30°C. Therefore the CMOS pixel detectors, such as Monolithic Active Pixel Sensors (MAPS) of ALPIDE family (ALice PIxel DEtector) which have high spatial resolution, speed and low power consumption will be used in the upgraded ALICE ITS [2].

Another strict requirement to reduce the multiple scattering effects and the detection threshold of the transverse momentum of charged particles implies minimizing the amount of low-Z materials within the sensitive area. This means that all parts of the upgraded ITS-silicon detectors, micro-cables, support structures and cooling system must contain a minimum amount of low-Z material. Up to now, the highest radiation transparency among all the current LHC experi-ments at the level of 1.1% X0 per layer, was achieved for the currently running ALICE ITS by application of the novel technology of the extra lightweight support structures with integrated cooling. The carbon fibre composite monolith structures (space frames up to 1200 mm length) providing thermo- and mechanically- stable support for three types of Si-detectors have been used [1, 2].

Another example of the low-mass technology is the Heavy Flavor Tracker (HFT) at STAR, where the material budget for two innermost $\sim$ 20 cm length layers is about 0.37% of a radiation length per layer [3].

The material budget of the upgraded ALICE ITS will be reduced by the use of ALPIDE chips. It will decrease the silicon material budget by a factor of seven per layer, in comparison to the present ITS (50 µm thick instead of 350 µm). Also a new electrical scheme will allow the material budget of the electrical power and signal cables to be reduced by a factor of five. Combining all these elements together, it should be possible for the first three layers (first three inner layers of new ITS) to build a detector with a radiation length of 0.3% X0 per single layer (including detectors, carbon fiber support structures with integrated cooling system and the electrical services) [2]. The power density on the pixel detectors (here the surface power density is used) has thus to be brought to a minimum and for the Inner Layers of the new ITS should not exceed 0.3 W/cm^2 [2]. In this paper, thermal tests of a single-phase liquid cooling system integrated in lightweight mechanical carbon fibre structures are presented. These structures were designed to ensure the requirements of a minimum material budget of three innermost layers of the new ALICE ITS [4–6].

2 Test samples

In the design of the ALICE ITS upgrade [1, 2] the very central part or Inner Barrel is assumed to be composed of three layers of 50 µm thick CMOS pixel detectors that will surround the interaction point. The detector (the ALPIDE Pixel Chip) has dimension 30×15 mm and contains pixel matrix consisted of 512×1024 sensitive pixels with sizes of 28×28 µm each. In the case of the mentioned three innermost layers, 9 Pixel Chips will be precisely positioned in a row and will be assembled on the Flexible Printed Circuit (FPC), forming the Hybrid Integrated Circuit (HIC). The HIC will be glued to the ultra-lightweight carbon fiber support structures of 290 mm length with embedded cooling pipes (figure 1).

These structures provide the functionality of the CMOS detectors in terms of operational temperature and mechanical position stability. They are composed of two main parts: a thin flat carbon fiber Cold Plate and an external support carbon fiber Space Frame. The first one will ensure the positioning and cooling of HICs of CMOS detectors. The Cold Plate is made of a high thermal conductive Carbon Fiber Reinforced Plastics (CFRP) in combination with different additional layers (see figure 2), with embedded cooling polyimide tubes providing the liquid coolant (water) circulation. The coolant inlet and outlet are provided by a connector at one end of the plate while at the opposite end the two polyimide tubes are joined by a U-bent connector. The heat from CMOS chips

2018 JINST 13 T08003

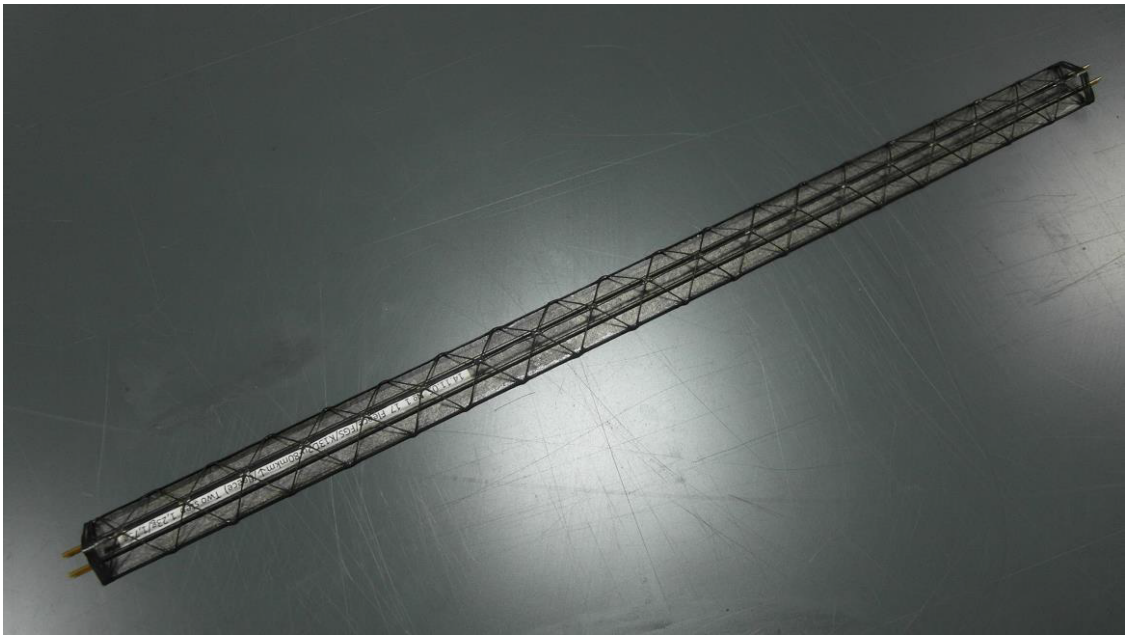

Figure 1. One of the ultra-lightweight carbon fiber support structures with integrated cooling system.

is conducted into the cooling pipes by the carbon fiber structure and is removed by the water flowing in the pipes [2, 4–6]. The HIC is glued to the Cold Plate in order to maximize the cooling efficiency.

The carbon fiber support Space Frame comprises a wound truss carbon fiber structure with a triangular cross section (obtained by winding a carbon rowing at an angle of 45° with respect to the Cold Plate longitudinal axis). It provides the mechanical stability of the whole linear module. For the Space Frame, the specific stiffness and the low-Z are the essential parameters driving the design. The carbon fiber with high Young's modulus (larger than 300 GPa) and with high thermal conductivity is used [2, 4–6].

All these ultra-lightweight Cold Plates and support structures are monolithic; they were made of carbon fiber composite in a single thermal polymerization process using manual lay-up and filament winding. After these two processes, the CFRP structure undergoes a curing process, needed for the polymerization, along with a pressure load. Gluing of different mechanical parts after curing has been minimized by assembling the CFRP structure before polymerization [2, 4–6]. In order to experimentally test the cooling performance of the carbon fiber support structures with embedded cooling arteries, five samples, based on the technologies reported in [4–7] have been used. The cross-sections and schematic layout (exploded view) of the studied samples are presented in figure 2.

For all samples the thermal conductive carbon fiber was oriented in the direction normal to the axis of the polyimide pipes. The samples differ in construction and in materials used to transfer heat from the HICs to the cooling pipes. All the information pertaining to the samples is summarized in a table 1. Various technologies for the major heat transfer elements, as well as several shapes and diameters of pipes, were tested in combination with different additional layers (see details in the table 1 and figure 2). For example for the samples 1, 3, 4 the layer of carbon paper enhances the heat transfer between the cooling channels and the plate (in case of round tubes). In the specimen with the flattened tubes (samples 2, 5) the carbon paper is removed and the heat transfer with the

2018 JINST 13 T08003

cold-plate is enhanced by the larger contact surface. The tubes are kept in the flattened prestressed configuration by the polymerized carbon laminate. Thus the optimization of competing factors, like heat transfer, material budget and mechanical stability might be achieved by selecting an optimal composition of materials, geometry and build-up technology. Therefore, samples 1-5 were studied in order to optimize the lay-up sequence for the Cold Plate and to choose the optimal design of these structures for the first three layers of ALICE ITS.

Table 1. Parameters of the samples of ultra-lightweight space support structures with integrated liquid cooling system.

Sample number	Material and thickness*	Number of plies	Dimensions of the cooling pipes and their geometry**	Weight (g)	Figure
1	1. Carbon fiber fleece 20 μm (down and top); 2. Carbon fiber plate 18 mm wide, mitsubishi K13D2U 70 μm 4. Carbon paper Amec Thermasol FGS 003 30 μm	4	round polyimide tubes, diameter 1.45 mm;	2.7	Figure 2(a)
2	1. Carbon fiber fleece 20 μm (down and top); 2. Carbon fiber plate 15.5 mm wide, mitsubishi K13D2U 70 μm	3	flattened polyimide tubes, diameter 1.45 mm;	2.1	Figure 2(b)
3	1. Carbon fiber fleece 20 μm (down and top); 2. Carbon fiber plate 18 mm wide, mitsubishi K13D2U 70 μm 4. Carbon paper Amec Thermasol FGS 003 30 μm	4	round polyimide tubes, diameter 1.02 mm;	1.8	Figure 2(c)

2018 JINST 13 T08003

4	1. Carbon fiber plate 15.5 mm wide, CF ThornelK1100X/CE2 90 μm 3. Carbon paper, CF paper FGS 003 30 μm 4. Carbon fiber fleece 20 μm	3	round polyimide tubes, diameter 1.02 mm;	2.0	Figure 2(d)
5	1. Carbon fiber plate 15.5 mm wide, CF ThornelK1100X/CE2 90 μm 3. Carbon fiber fleece 20 μm	2	flattened polyimide tubes, diameter 1.45 mm;	1.6	Figure 2(e)

*for all samples the orientation of fibers = 90° to the polyimide cooling pipe

**for all Samples the cooling pipes wall thickness is 25 μm

3 Experimental testing of cooling performance

A special test facility was developed for carrying out the experimental thermal tests of the ultra-lightweight support structures (Samples) described in section 2. The aim of these tests is to check the efficiency of the carbon fiber panels in terms of heat removal capabilities using special heaters to simulate the detector chips mounted on these panels.

The test facility was located in a temperature-controlled room including manifolds for water feeding, temperature and pressure sensors and the data acquisition system. The pressure of the cooling water was monitored with two input instruments: a dial gauge (rough measurement) and a pressure sensor MPX2200GP. The readings from the pressure sensor were recorded in a computer. The water pressure was regulated within 0.3 bar. Pressure monitoring was carried out in all the measurements.

Each sample was heated by a polyimide heater, which simulates heat load from the real detector. The samples were tested in air for the detector power densities of 0.3, 0.4 W/cm^2, as well as 0.1 W/cm^2 and 0.5 W/cm^2 as the lower and the upper limits, respectively. A small portion of the applied power is exchanged directly with the environment by convective and radiation heat transfer. This has been estimated by measurements of water flow and temperature difference between sample inlet-outlet water channels. It was obtained that for different samples the 85%–90% heat transfer goes to the water, while the rest part of the heat can be exchanged with the environment.

The Polyimide (Kapton) flexible heater (was manufactured for the present measurements) is a flat strip, 290 mm long, 14 mm wide. It has standard structure: thin dielectric polymer film (100 μm

2018 JINST 13 T08003

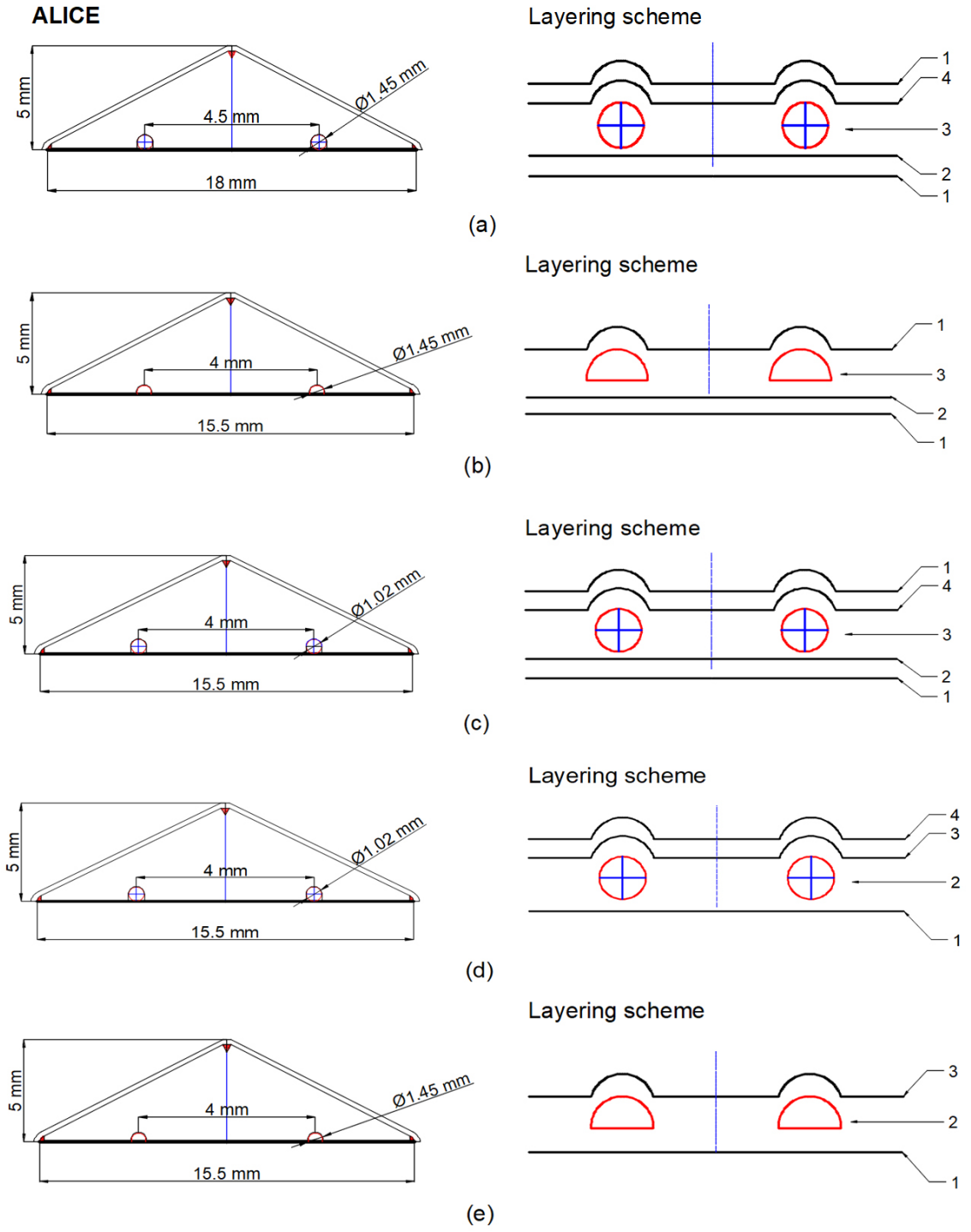

Figure 2. Figure 2. Layout of the investigated samples of ultra-lightweight space support structures with integrated liquid cooling system. Left: cross-section of the Cold Plate and Space Frame. Right: schematic layout (exploded view). (a) Sample 1; (b) Sample 2; (c) Sample 3; (d) Sample 4; (e) Sample 5. For more information see the text.

polyimide), encapsulated with a thin conductive foil inside (resistive heating element) and fed with a fixed electrical current.

In each sample, the heater was glued with thermal grease to the carbon fiber panel. Thermal grease is a combination of polydimethylsiloxane (silicone oil), fumed silica (thickener) and zinc oxide (thermally conductive filler). The main properties are: thermal conductivity $\sim 0.7\,\mathrm{W{\cdot}m^{-1}{\cdot}K^{-1}}$; density $\sim$ 2.6–3.0 $\mathrm{g{\cdot}cm^{-3}}$. The thickness of grease layer between heater and the samples was approximately 0.05 mm. The quality of the thermal contact of the heater with the test samples and information regarding the homogeneity of the power dissipation was obtained by using of the infrared (IR) camera. It mapped the heater temperature at low power densities allowing the information about the temperature homogeneity of the whole sample.

For more precise measurements of the sample thermal characteristics the five thermocouples were installed on the heater to read out local temperatures. These thermocouples were inserted (in vertical position) into the special platform. The last one was able to move along the entire surface the sample. Thus the position of the thermocouples was changed to perform the measurements at the center line or at the edges of the Cold Plate. The distance between the thermocouples was 65 mm, and the temperature map of 15 points required 3 subsequent measurements under well controlled stable conditions. The accuracy of the thermocouples fixation at the same position on the sample surface was about ±0.3 mm. Thermal contact of all thermocouples (thermocouples were rigidly fixed and didn't move during the measurements) with the surface of the sample was ensured by application of a thermal grease. During the experiment the thermocouples are located either at the center of the heater: position 2, figure 3(a); or along the edge of the heater with the water outlet side (water drain from the sample): position 3, figure 3(b), or along the edge with the water inlet side (water intake into the sample): position 1, figure 3(c). Since some samples have different widths (see the table 1) in case of the measurements along the edges of the heater (position 3 in figure 3(b), position 1 in figure 3(c)) the thermocouples were attached always at the edge (about 1 mm from the edge) of the cooling plate regardless of the total width.

As a result, a temperature field of the entire sample surface was obtained. Thermocouples with associated electronics were calibrated against three temperatures: 0°C (thermostat with melting ice); 50°C (thermostat with hot water); 11°C (thermostat with cold water). The result of the calibration procedure is that the difference between temperature measured by a reference thermometer (with an accuracy of ±0.1°C): T_{ref} and temperature (average) measured by thermocouples: $T_{tcouple}$. ($T_{ref} - T_{tcouple}$) was about zero. During all the measurements the readings from the thermocouples were averaged (statistical error) and the deviation from the mean values was less than ±0.4°C. From these estimations one can conclude that the error of the measurements is lower than ±0.4°C.

Also the adjustment of the five thermocouples on the heater was performed before each measurement in order to verify the reliability of the thermal contact between thermocouples and the heater. For this purpose, the heater temperature was measured when the heater is off and the water supply is on. In this case, the thermocouples must read out a temperature value similar to the inlet water temperature. The difference between the maximum and minimum readings by the thermocouples was required not to exceed ±0.4°C. After the measurements, when the sample was cooled (the heater turned off), the readings from the thermocouples were checked to determine whether they provide the same temperature as at the beginning of the measurements. This condition was fulfilled in all experimental cases.

2018 JINST 13 T08003

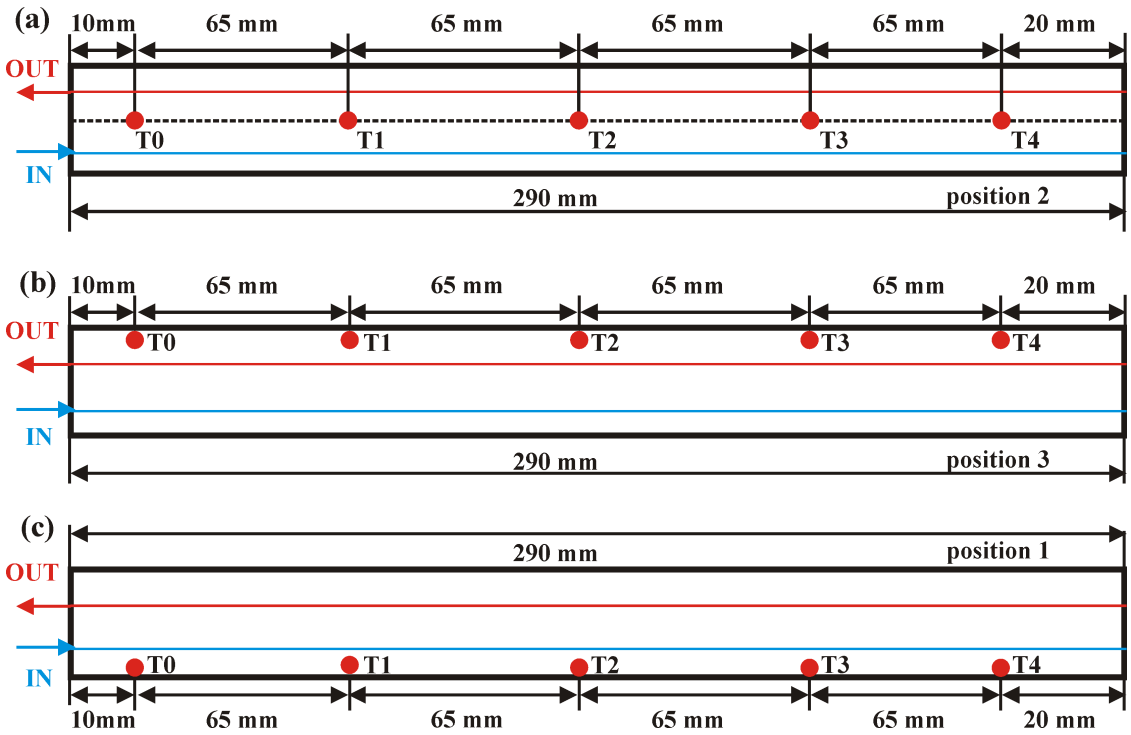

Figure 3. Location of the thermocouples on the heated sample surface: (a) at the centerline of the heater; (b) at the edge of the heater with the outlet water tube; (c) at the edge of the heater with the inlet water tube.

Two additional thermocouples were used to measure the temperature of the ambient air. All these thermocouples were connected to an *ad-hoc* designed electronic device (an amplifier and an analog-to-digital converter), which includes a data acquisition and processing system. The output information from this electronic device was read out into a personal computer. Another two thermocouples measured the water temperature in the inlet and outlet tubes(the range of the temperature at the inlet used for the different tests is 10–15°C of the sample cooling system. Since these thermocouples were of a different type, they were connected to a separate data acquisition system. Both thermocouples were mounted firmly on the metal adapters providing water intake and drain to the sample (the values of a temperature and the temperature difference between the inlet and outlet water have been obtained). The monitoring of the water flow was carried out by a flow meter.

Experimental studies were carried out in order to select the optimal design of the cooling and support structure complying with the criterion of a minimum material budget, without exceeding the temperature on the heater: 30°C at 0.5 W/cm^2 (surface power density). This parameter is important for the optimal performance of Monolithic Active Pixel Sensors (there is no temperature limit for heater operation at used power densities, but for MAPS operability the upper temperature limit is 30°C). These criteria were used in the selection of the support structure with the most efficient liquid cooling system.

Thermal tests were carried out for five extremely lightweight samples, which differ in both design and technological parameters (see figure 2 and table 1). The tests were performed at heater power densities of 0.1, 0.3, 0.4 and 0.5 W/cm^2 keeping in mind expected power density and associated safety factors. An optimal inlet water pressure was selected to be in the range of

2018 JINST 13 T08003

0.30–0.35 bar. The water flow rate is fixed at 3 l/h. The tests results were compared with the test campaign performed at CERN [8–11].

4 Results

The temperature distribution along each sample (temperature profile) was reported using five thermocouples readings (as described above). Figure 4 shows the normalized temperature (the difference between temperature at the current point of the sample and the inlet water temperature, i.e. normalization on the inlet water temperature) distribution along the samples at 0.5 W/cm^2 power density. This temperature profile was obtained from therefore the thermocouples mounted on central stave line (see figure 3(a)). All data uncertainties are not more ±0.4°C and for all plots they are smaller than the symbol size. According to the plot, the best thermal performance is obtained for the most massive sample 1 (see illustration for this sample in figure 2 and table 1), equipped with the large round polyimide tubes with the inner diameter (ID) 1.45 mm. Sample 2, also fairly massive and equipped with 1.45 mm ID flattened polyimide tubes (see figure 2 and table 1), displays the second best thermal performance. Sample 3 with tubes of 1.02 mm, is representing the best compromise between material budget optimization and structure stability. It shows a slightly larger temperature. The heat removal from samples 4 with the tubes of 1.02 mm ID, and sample 5 with flattened tubes show a cooling performance at about the same level as sample 2.

The main conclusion from these results is that the structures with minimum lay-ups and with small tubes diameter (see the table 1 for samples 4 and 5) provide a similar cooling performance as the more massive samples (see the table 1 for samples 1, 2). With an optimal pressure and cooling water flow, a significant power density (0.5 W/cm^2) could be dissipated from the sample by the cooling water yielding the operational temperature below 30°C, for a water inlet temperature of 11°C.

For samples 4 and 5, which showed a similar thermal performance, a more detailed study of the surface temperature profiles was performed. As illustrated in figure 5, three temperature profiles per sample were obtained by using five thermocouples installed as illustrated in figure 3 (i.e. points in figure 5 are located at distances: 10 mm, 75 mm, 140 mm, 205 mm, 270 mm from the sample inlet-outlet water channel), for power density values of 0.1, 0.3, 0.4 and 0.5 W/cm^2.

Analysis of the data shown in figure 5 reveals that the temperature of the sample does not exceed 24°C at 0.3 W/cm^2 for a water inlet temperature of 14°C. This result is within the normal operation mode of the detector, not exceeding 30°C). For sample 4 it can be clearly seen that, at power densities up to 0.3 W/cm^2, the temperature profile is fairly uniform; temperature deviations do not exceed 2°C. Significant temperature deviations appear at power densities above 0.4 W/cm^2, and in all cases the central region is the hottest.

For sample 5, the situation is similar — at power densities up to 0.4 W/cm^2, deviations in temperatures are almost minimal, indicating the quality and cooling uniformity in all areas of the sample. Moreover, for the sample 5 at 0.5 W/cm^2 the deviations in temperatures in its central region (with the exception of some points in the edge areas) are also minimal. It should be noted that the same results were obtained for the sample 3 with round tubes of 1.02 mm diameter. Details of these edge effects become evident when studying the temperature field of sample 5 from other measurements, for example test in reverse geometry (in this case the flow direction of the coolant was changed to opposite). The corresponding results are shown in figure 6, where one of the

2018 JINST 13 T08003

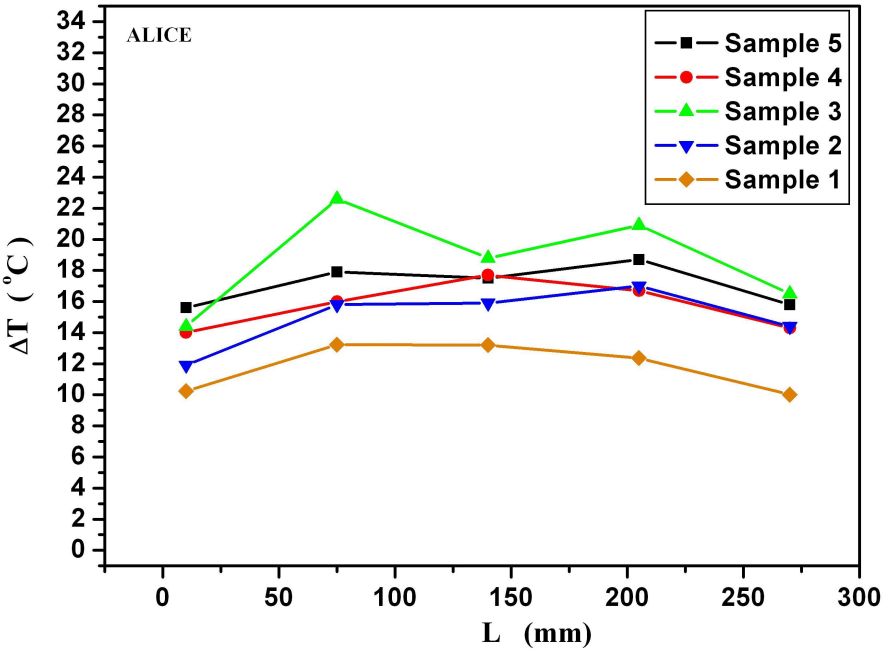

Figure 4. Normalized temperature profiles along the samples (at the central stave line). The vertical axis shows the difference between the temperature of the current point of the sample and the measured temperature of the inlet water. The heating power density was 0.5 W/cm^2.

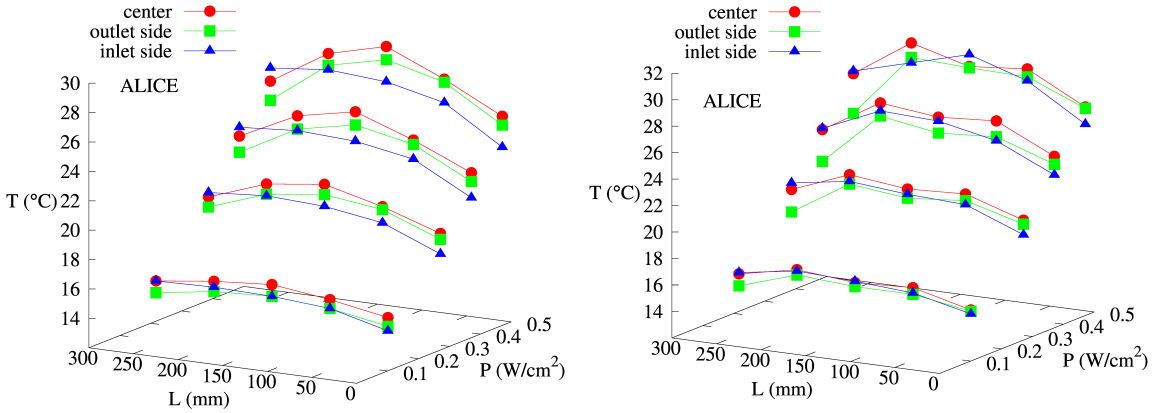

Figure 5. Temperature profile of the sample 4 (a) and sample 5 (b) at: 0.1, 0.3, 0.4 and 0.5 W/cm^2 power densities. Red dots — thermocouples located in the middle of the heater, green dots — thermocouples located on the edge of the heater close to the inlet channel (temperature 14°C) side, blue dots — thermocouples arranged along the edge of the heater close to outlet water channel.

axes indicates the location of the thermocouples across the sample: positions 1–3. Position 3 — thermocouples mounted on the edge of the heater towards the inlet water channel (see figure 3(c) for illustration), position 2 — thermocouples mounted in the middle of the heater (figure 3(a)), position 3 — thermocouples mounted along the edge of the heater close to the outlet water channel

2018 JINST 13 T08003

(see figure 3(b)). The other two axes represent the applied power density (0.1, 0.3, 0.4 and 0.5 W/cm^2) and the difference between the measured sample temperature and the temperature of the inlet water. The temperature measurements were recorded along thesample (as shown in figure 3).

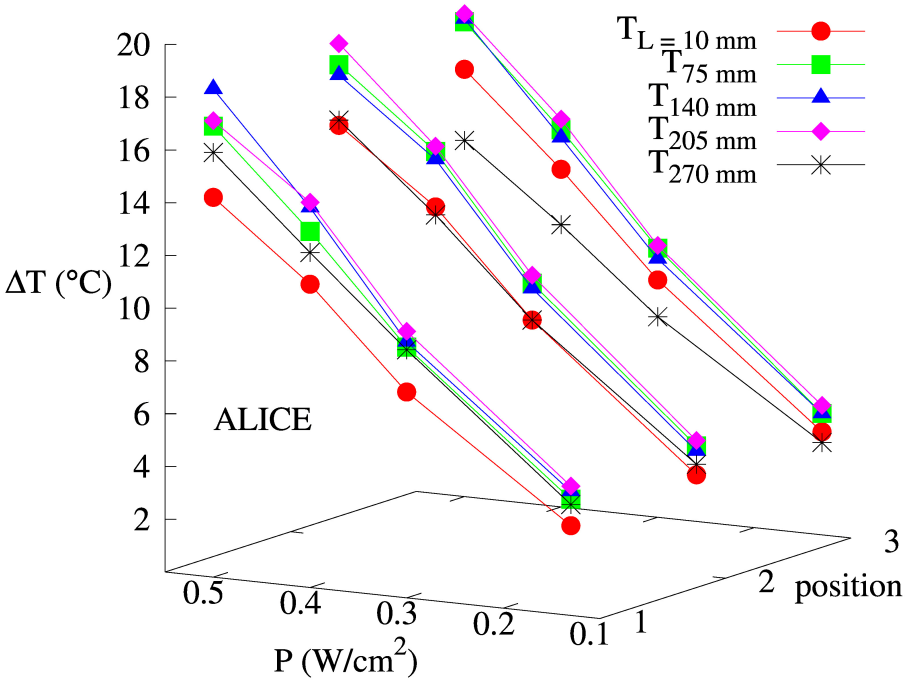

Figure 6. Normalized heater temperature profiles of sample 5 power densities of: 0.1, 0.3, 0.4 and 0.5 W/cm^2. Arrangement of thermocouples (positions 1–3) across the sample is shown. Here, the location of the thermocouples on the heated sample surface: $T_{L=10\,mm}$,$T_{75\,mm}$, $T_{140\,mm}$, $T_{205\,mm}$, $T_{270\,mm}$ corresponds to the location of the thermocouples: T0, T1, T2, T3, T4 shown in figure 3. The vertical axis shows the difference between the temperature of the current point of the sample and the measured temperature of the inlet water.

From the distribution shown in figure 6 it can be seen that larger temperature gradients occur at the extremities when applying a power density of 0.5 W/cm^2, particularly at the longitudinal edges of the sample (see measurements in positions 1 and 3 in figure 6). In the center of the sample (position 2) the temperature profile is fairly uniform. Thus, it can be concluded that the different thermal effects (the local overheating areas have been observed) associated to structural features and material layup of the samples appear when power density exceeds 0.4 W/cm^2. One of the possible explanation of such effects may be associated with the inhomo-geneities of the thermal conductive carbon fiber materials, which arose at manufacturing of the Cold Plate. It would be interesting to investigate further more samples with different material layup and material budget (different geometrical size, different polyimide tubes, etc) of the Cold Plate. For the minimum material budget sample (sample 5), no significant increase in the centerline-edge temperature field was observed with respect to more massive samples (sample 3 or 4), indicating that uniform cooling capabilities are preserved even in the lighter stave layup. To determine the warmest area on the sample, temperature profiles were recorded at different power densities. The results are shown in figures 7, 8 and 9 for the power density of 0.3 W/cm^2 for samples 3, 4 and 5, respectively. As in figure 6, the axis named 'position' corresponds to the location of thermocouples on the heated surface, indicated by the black dots.

2018 JINST 13 T08003

An analysis of the temperature profiles of the samples shows that there is a uniformly heated area (poorly cooled region) at the center of the samples 3 and 4 (see figure 7 and figure 8) and good uniform cooling of the peripheral areas of the samples. Sample 5 (see figure 9), displays a warmer region at 250 mm, while the rest of the sample remains well cooled.

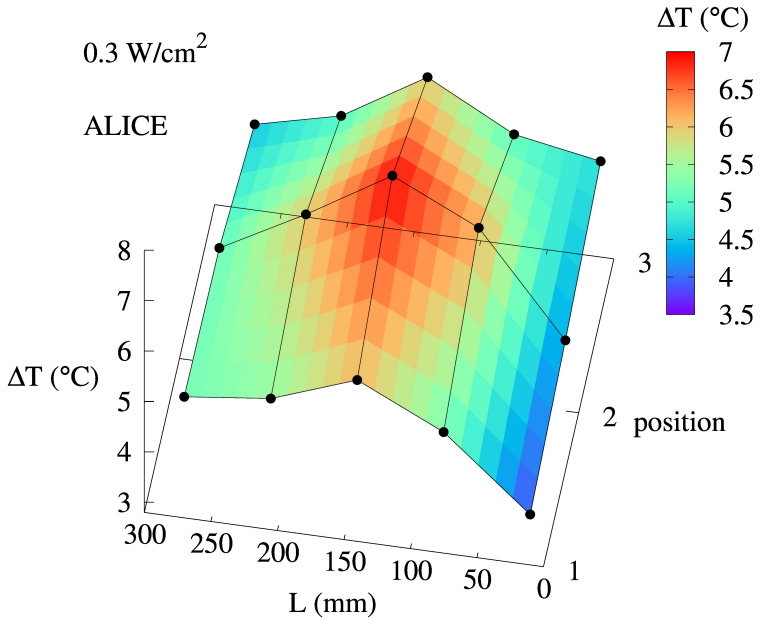

Figure 7. Normalized temperature profile of sample 3. Arrangement of thermocouples (positions 1-3) across the sample is shown.

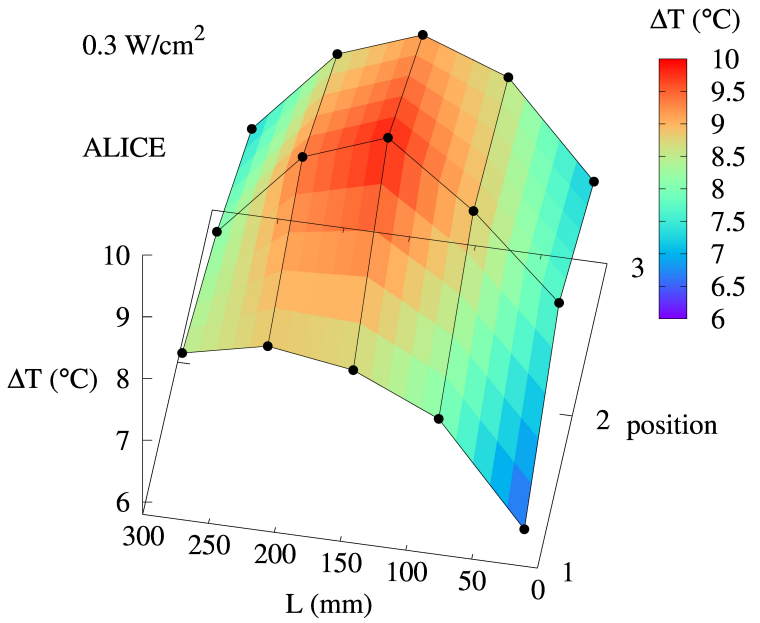

Figure 8. Normalized temperature profile of sample 4. Arrangement of thermocouples (positions 1–3) across the sample is shown.

2018 JINST 13 T08003

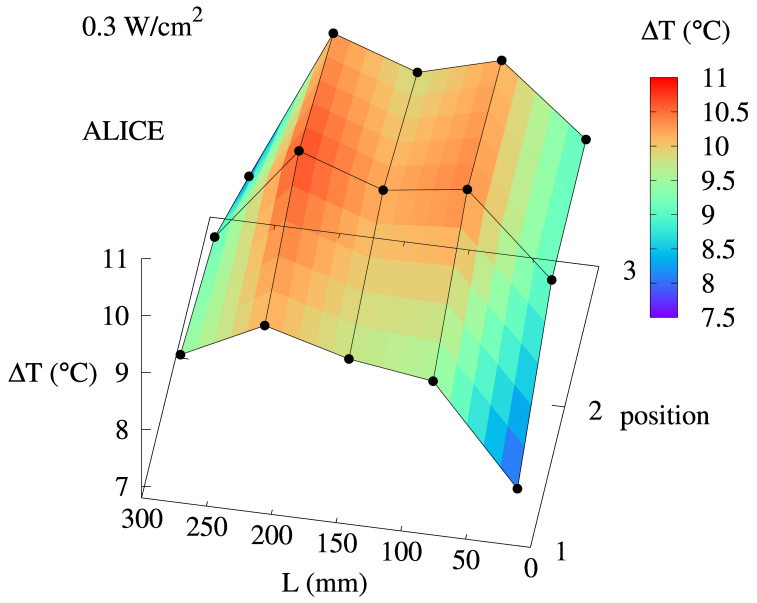

Figure 9. Normalized temperature profile of sample 5. Arrangement of thermocouples (positions 1–3) across the sample is shown.

Further studies of the temperature profiles with increased power densities of up to 0.5 W/cm^2 showed additional regions with local overheating in sample 5. As a result of the performed measurements the samples 3 and 4 demonstrate the best characteristics among other samples in cooling performance (e.g. round pipe instead of flattened in sample 5), mechanical stability and material budget. Besides, sample 3 has at the same power density 0.3 W/cm^2 a small region of local over-heating (in comparison with the other samples) and also sample 3 has the smallest temperature in this region. Therefore, sample 3 has been selected for the ALICE ITS upgrade as ultra-lightweight structure featuring the best compromise between thermal performance, material budget (lower than sample 4, i.e. K13D2U 0.07 mm vs CF Thornel K1100X/CE2 0.09 mm), mechanical stability (round polyimide tubes instead of flattened tubes as in sample 5) and easy manufacturing (K13D2U is used instead of Thornel K1100 that is more expensive and not easy to find). This choice is further justified by the lower heat dissipation, below 0.1 W/cm^2, associated to the recent development of the final detectors design.

5 Conclusions

Several ultra-lightweight carbon fiber structures with different designs were tested. The structures combine high cooling performance and thermomechanical stability with minimum material inventory. This provides a record radiation transparency of 0.3% X_0 for the whole detection layer and all services. Tests results confirmed that using of such structures a significant heat load from the whole set of silicon detectors (up to 26 W per 30 cm stave) can be removed. Thus, the new developed ultra-lightweight support structures with the integrated cooling system can successfully be used in upgrades of the inner trackers in experiments to study the new physics at the Large Hadron Collider. On the other hand, with decreasing heat dissipation of the future detector systems we could construct

2018 JINST 13 T08003

new ultra-lightweight carbon fiber structures without cooling system (without polyimide tubes with liquid coolant) to reduce the material budget. These structures can also be used in the future vertex detectors planned for experiments NA61 (SHINE) at the SPS in CERN [12], at FAIR at GSI in Darmstadt [13] and at MPD-NICA at JINR in Dubna [14, 15].

Acknowledgments

This work was supported for the SPbSU participants within the Program of Russian groups activities in the ALICE upgrade by the Ministry of Education and Science of Russian Federation, contract No. 14.610.21.0003, identification number RFMEFI61014X0003 (SPbSU identification number No. 11.19.1632.2014).

The reported study was supported by RFBR, research project No. 15-32-20546.

V.I. Zherebchevsky would like to thank St.-Petersburg State University for grants No. 11.42.684.2017 and 11.40.531.2017.

References

[1] ALICE collaboration, *Conceptual Design Report*, CERN-LHCC-2012-013, LHCC-P-005, 2012.

[2] ALICE collaboration, B. Abelev et al., *Technical Design Report for the Upgrade of the ALICE Inner Tracking System*, *J. Phys.* **G 41** (2014) 087002.

[3] D. Beavis et al., *The STAR Heavy Flavor Tracker Technical Design Report*, https://drupal.star.bnl.gov/STAR/starnotes/public/sn0600, 2011.

[4] C. Gargiulo et al., *Studies on the composite light structure for the ALICE Silicon tracker upgrade*, talk given at *Forum on tracker detectors mechanics*, CERN, Geneve, Switzerland, July 2012.

[5] C. Gargiulo et al., *Studies on the mechanics and cooling of the ALICE ITS upgrade based on carbon fibre structures*, talk given at *Forum on tracker detectors mechanics*, Desy, Hamburg, Germany, July 2014.

[6] C. Gargiulo et al., *Lightweight Thermomechanical structures*, talk given at 2^{nd} *ECFA High Luminosity LHC Experiments Workshop*, Aix-les-Bains, France, October 2014.

[7] V.I. Zherebchevsky, S.N. Igolkin, E.B. Krymov, N.A. Maltsev, N.A. Makarov and G.A. Feofilov, *Extra lightweight mechanical support structures with the integrated cooling system for a new generation of vertex detectors*, *Instrum. Exp. Tech.* **57** (2014) 356.

[8] M. Gomez Marzoa, M. Battistin, C. Bortolin, J.A.B. Direito, E. Da Riva, C. Gargiulo et al., *Thermal studies of an ultra-low-mass cooling system for ALICE ITS upgrade project at CERN*, talk given at 8^{th} *World Conference on Experimental Heat Transfer, Fluid Mechanics, and Thermodynamics*, Lisbon, Portugal, June 2013.

[9] M. Gomez Marzoa and C. Gargiulo. *Thermal performance of lightweight cooling systems for the ALICE ITS Upgrade*, talk given at *Forum on tracker detectors mechanics*, Desy, Hamburg, Germany, June 2014.

[10] A. Francescon, G. Romagnoli, A. Mapelli, P. Petagna, C. Gargiulo, L. Musa et al., *Development of interconnected silicon micro-evaporators for the on-detector electronics cooling of the future ITS detector in the ALICE experiment at LHC*, talk given at 4^{th} *Micro and Nano Flows Conference UCL*, London, U.K., September 2014 [*Applied Thermal Engineering* **93** (2016) 1367].

2018 JINST 13 T08003

[11] G. Fiorenza, V. Manzari, C. Pastore, I. Sgura, M. Torresi and C. Gargiulo, *An innovative polyimide microchannels cooling system for the pixel sensor of the upgraded ALICE inner tracker*, in proceedings of *5th IEEE International Workshop on Advances in Sensors and Interfaces IWASI*, Bari, Italy, 2013, pp. 81–85.

[12] NA61/SHINE collaboration, *Report from the NA61/SHINE experiment at the CERN SPS, Status report to the proposal SPSC-P-330*, https://cds.cern.ch/record/2287091.

[13] T. Ablyazimov, A. Abuhoza, R.P. Adak, M. Adamczyk, K. Agarwal, M.M. Aggarwal et al., *Challenges in QCD matter physics — The scientific programme of the compressed baryonic matter experiment at FAIR*, *Eur. Phys. J.* **A 53** (2017) 60.

[14] K. Abraamyan, S. Afanasiev, V. Alfeev, N. Anfimov, D. Arkhipkin, P. Aslanyan et al., *The MPD detector at the NICA heavy-ion collider at JINR*, *Nucl. Instrum. Meth.* **A 628** (2011) 99.

[15] V.D. Kekelidze, V.A. Matveev, I.N. Meshkov, A.S. Sorin and G.V. Trubnikov, *Project nuclotron-based ion collider fAcility at JINR*, *Phys. Part. Nuclei* **48** (2017) 727.

2018 JINST 13 T08003